Actin Filament Organization in the Fish Keratocyte Lamellipodium

J. Victor Small, Monika Herzog, and Kurt Anderson

Institute of Molecular Biology, Austrian Academy of Sciences, A-5020 Salzburg, Austria

Abstract. From recent studies of locomoting fish keratocytes it was proposed that the dynamic turnover of actin filaments takes place by a nucleation–release mechanism, which predicts the existence of short (less than 0.5 μm) filaments throughout the lamellipodium (Theriot, J. A., and T. J. Mitchison. 1991. *Nature (Lond.).* 352:126–131). We have tested this model by investigating the structure of whole mount keratocyte cytoskeletons in the electron microscope and phalloidin-labeled cells, after various fixations, in the light microscope.

Micrographs of negatively stained keratocyte cytoskeletons produced by Triton extraction showed that the actin filaments of the lamellipodium are organized to a first approximation in a two-dimensional orthogonal network with the filaments subtending an angle of around 45° to the cell front. Actin filament fringes grown onto the front edge of keratocyte cytoskeletons by the addition of exogenous actin showed a uniform polarity when decorated with myosin subfragment-1, consistent with the fast growing ends of the actin filaments abutting the anterior edge. A steady drop in filament density was observed from the mid-region of the lamellipodium to the perinuclear zone and in images of the more posterior regions of lower filament density many of the actin filaments could be seen to be at least several microns in length.

Quantitative analysis of the intensity distribution of fluorescent phalloidin staining across the lamellipodium revealed that the gradient of filament density as well as the absolute content of F-actin was dependent on the fixation method. In cells first fixed and then extracted with Triton, a steep gradient of phalloidin staining was observed from the front to the rear of the lamellipodium. With the protocol required to obtain the electron microscope images, namely Triton extraction followed by fixation, phalloidin staining was, significantly and preferentially reduced in the anterior part of the lamellipodium. This resulted in a lower gradient of filament density, consistent with that seen in the electron microscope, and indicated a loss of around 45% of the filamentous actin during Triton extraction.

We conclude, first that the filament organization and length distribution does not support a nucleation release model, but is more consistent with a treadmilling-type mechanism of locomotion featuring actin filaments of graded length. Second, we suggest that two layers of filaments make up the lamellipodium; a lower, stabilized layer associated with the ventral membrane and an upper layer associated with the dorsal membrane that is composed of filaments of a shorter range of lengths than the lower layer and which is mainly lost in Triton.

To move over a natural or synthetic substrate, metazoan cells protrude a thin layer of cytoplasm, a lamellipodium, that establishes new anterior contacts required for forward locomotion (see review by Heath and Holifield, 1991). The lamellipodium is thus the primary locomotory organelle (Abercrombie et al., 1970), but its gross movements are invariably irregular; in the light microscope it commonly shows complex forward, backward, and folding motions, so that net progress may appear rather erratic. Various lines of evidence indicate that lamellipodial movements are governed by a continuous remodeling of the cytoskeleton, specifically of actin filaments. Protrusion has been directly correlated with the formation of a dense, laminar network of actin filaments (Rinnerthaler et al., 1991) that make up the core of the lamellipodium (Höglund et al., 1980; Small, 1981, 1988) and experiments on fibroblasts injected with labeled actin probes, indicate that there is a dynamic turnover of actin filaments in the lamellipodium, involving polymerization at the front and depolymerization at the rear (Wang, 1985; Okabe and Hirokawa, 1989; Forscher and Smith, 1988; Symons and Mitchison, 1991).

Although the involvement of actin filaments in protrusive activity is now more or less accepted, there are still many open questions and conflicting ideas about how movement occurs (see also reviews by Oster and Perelson, 1987; Mitchison and Kirschner, 1988; Smith, 1989; Small, 1988; Heath and Holifield, 1991; Lee et al., 1993; Condeelis, 1993): can actin polymerization alone produce movement or are the myosin motors that are found in lamellipo-

Address all correspondence to J. V. Small, Institute of Molecular Biology, Austrian Academy of Sciences, Billrothstrasse 11, A-5020 Salzburg, Austria. Tel.: (43) 662 63961-11. Fax: (43) 662 63961-40.

dia (Fukui et al., 1989; Wagner et al., 1992) also required and, if so, what are the mechanisms involved? How is the assembly and disassembly of actin spatially regulated and does disassembly occur by endwise depolymerization or by severing? How are actin subunits transported to the front of the lamellipodium to support filament growth, against the direction of cytoskeletal flow? Further, what roles do actin-binding proteins play in regulating the dynamic changes of cytoskeletal architecture in vivo (see e.g., Carlier and Pantoloni, 1994; Theriot, 1994; Zigmond, 1993; Stössel, 1993). These considerations prompt also the more general question of how the actin filaments are in fact organized in the lamellipodium: what is their length, polarity, and orientation? It is the latter problem that will form the focus of the present report.

In earlier studies on fibroblast cytoskeletons (Small and Celis, 1978; Small et al., 1978, 1982; Small, 1981, 1988) prepared by the negative staining method, it was shown that the lamellipodium consists of a criss-cross network, or weave (Höglund et al., 1980) of actin filaments whose fast growing, barbed ends were directed towards the leading membrane. In fibroblasts as well as in other cells (Edds, 1977; Höglund et al., 1980; Karlsson et al., 1984; Rinnerthaler et al., 1991) the angle of orientation of filaments relative to the membrane was variable and, in addition, bundles of filaments (microspikes) were commonly found that traversed the lamellipodium from front to back and that appeared to arise from a lateral coalescence of the filaments in the networks. Owing to the high density of the filament networks it was difficult to measure individual filament lengths, but from the presence of filaments in small, parallel or splayed arrays and the observed interrelationship between the networks and the microspike bundles, it was apparent that many actin filaments were long, extending from the front to the rear of the lamellipodium, (see also Small, 1994). In contrast, other studies, using alternative methods, revealed only short filaments. Thus, using the quick-freeze deep-etch procedure, the length of filaments in macrophages was estimated to be in the range of 0.5 μm (Yin and Hartwig, 1988) and using a kinetic approach, Cano et al. (1991) deduced an average filament length in leukocyte lysates of 0.3 μm. Lewis and Bridgman (1992) using both negative staining and freeze-drying observed two populations of actin filaments in nerve growth cones, both long and short and of different polarities relative to the cell front.

A reconsideration of the problem of filament length was stimulated by the work of Theriot and Mitchison (1991) on fish keratocytes. The latter cells are particularly suitable for locomotion studies since they show rapid (rate around 10 μm/min) persistent forward movement that is driven by a broad and thin, fan-shaped lamellipodium (Goodrich, 1924; Cooper and Schliwa, 1986). Using a caged fluorescent derivative of actin, Theriot and Mitchison (1991) showed, significantly, that the actin filament cytoskeleton of the keratocyte lamellipodium is stationary relative to the substrate as the cell moves. Such a result is consistent with treadmilling of actin filaments, with growth at the front of the lamellipodium and depolymerization at the rear. However, Theriot and Mitchison made two further observations that, together could not be reconciled with a treadmilling model. They noted that there was an exponential decay of activated actin fluorescence intensity from the front to the rear of the lamellipodium in living cells that did not parallel the actin filament density as determined by phalloidin staining of fixed cells which, in their preparations, was uniform across the lamellipodium. Accordingly, they proposed a nucleation–release model of cell locomotion (Theriot and Mitchison, 1991, 1992*a*) which predicts a non-oriented organization of short filaments, throughout the lamellipodium of <0.5 μm in length. We have now tested this model by investigating the structural organization of the keratocyte cytoskeleton. Our results indicate that there is a steep gradient of filament density across the lamellipodium, that the filaments are graded in length and are organized in a more or less regular two-dimensional lattice. Taken together with Theriot and Mitchison's results on the decay of activated fluorescence (1991), the data supports a treadmilling-type mechanism of locomotion. At the same time, the existence of an extra filament component is highlighted that is readily lost during Triton extraction and that may derive from the dorsal side of the lamellipodium complex.

Materials and Methods

Cells

Keratocytes were prepared from the scales of the golden trout (*Salmo alpinus*) using modifications of the techniques described by others (Kolega, 1986; Cooper and Schliwa, 1986). Scales removed from freshly slaughtered fish were transferred to DME and then to fish Ringer solution (112 mM NaCl, 2 mM KCl, 2.4 mM NaH CO_3, 1 mM $CaCl_2$, 1 mM Tris, pH 7.3) containing 0.5 mg/ml collagenase (type V; Sigma Chem. Co., St. Louis, MO) for 5 to 7 min at room temperature. After rinsing in DME, the scales were rinsed once and stored in a culture medium, "start medium", comprised of a mixture of fish Ringer (70%), DME (20%), and Steinberg medium (10%) supplemented with 10 mM Pipes, pH 7.5, and 2% chicken serum. The Steinberg medium contained 52 mM NaCl, 0.3 mM Ca $(NO_3)_2/H_2O$, 0.6 mM KCl, and 0.8 mM $MgSO_4/6$ H_2O.

For electron microscopy, tissue was removed from the scales with fine needles under a dissecting microscope and transferred to a carbon-formvar–coated gold or nickel electron microscope grid (150 mesh, hexagonal; Science Services, Munich, Germany) mounted in a drop of start medium on a 10-mm diam coverslip. The tissue piece was held against the grid by overlaying a second small coverslip (4 × 4 mm) and the resulting sandwich was transferred to a petri dish containing a layer of moist filter paper in the lid. The preparations were kept at room temperature and periodically replenished with a small drop of medium, as required. When cells had moved out from the explants (after 1 to 3 h) the coverslip sandwich was transferred to a "running" medium composed of 90% fish Ringer, 10% Steinberg medium, 10 mM Pipes, pH 7.0, and gently dismantled. Grids and coverslips carrying cells were kept in this medium, sometimes supplemented with a few drops of start medium, ready for use.

For video-microscopy of live cells, cells were grown on 20-mm diam glass coverslips using essentially the same procedure as above, with the tissue pieces sandwiched between the large coverslip and a 4 × 4 mm coverslip.

Preparation of Cytoskeletons and Negative Staining

For electron microscopy, cells were extracted at room temperature in modified fish Ringer solution (MFR[1]: 112 mM NaCl, 2 mM KCl, 2.4 mM $NaHCO_3$, 2 mM $MgCl_2$, 5 mM EGTA, 10 mM MES, pH 6.1) containing 0.5% Triton X-100 for 15 s. They were then fixed for 15 min in 1% glutaraldehyde in the same buffer and subsequently incubated with phalloidin (10 μg/ml in MFR) for 10–15 min prior to negative staining with aqueous 2% sodium silicotungstate (see Small, 1981) or a 1:1 mixture of 2% sodium silocotungstate and 2% phosphotungstic acid. In some cases, ex-

1. *Abbreviations used in this paper*: MFR, modified fish Ringer; S-1, subfragment-1.

traction in Triton X-100 was followed by incubation with 0.5 mg/ml smooth muscle tropomyosin in MFR (before the fixation step) to add stability to the actin filaments. Electron microscopy was carried out using a ZEISS EM 10 A electron microscope.

Actin Polymerization and S-1 Labeling

Actin was purified from skeletal muscle acetone powder essentially according to Spudich and Watt (1970). Myosin subfragment-1 (S-1) was prepared from rabbit skeletal muscle myosin according to Okamoto and Sekine (1985). To produce actin fringes on keratocyte cytoskeletons, for myosin S-1 decoration at the cell front, the following steps were used. Cytoskeletons were prepared as above but were fixed only briefly for 2 min in 0.1% glutaraldehyde in MFR. After rinsing, they were incubated in phalloidin (10 μg/ml in MFR) for 3 min, rinsed in cold actin polymerization buffer (APB: 112 mM KCl, 4 mM $MgCl_2$, 3 mM EGTA, 10 mM Pipes, pH 6.8) and incubated on ice for 2 min with 0.8 μM G-actin diluted from a 100× stock into APB. They were then rinsed again (in APB), treated with phalloidin in MFR a second time, as above, rinsed in S-1 buffer (0.1 M KCl, 10 mM Tris/HCl, pH 7.0) and incubated with 0.5–1 mg/ml S-1 in the same buffer for 30–60 s at room temperature. Following a rinse in S-1 buffer the grids were transferred to a mixture of 1% glutaraldehyde and 0.05 mg/ml tannic acid (in MFR) for 5 min and then to MFR. After washing with a few drops of a spreading solution (Moore et al., 1970) containing 0.5 mg/ml cytochrome C, 0.1% amyl alcohol, the grids were negatively stained in 1% aqueous uranyl acetate. To reduce unwanted background at

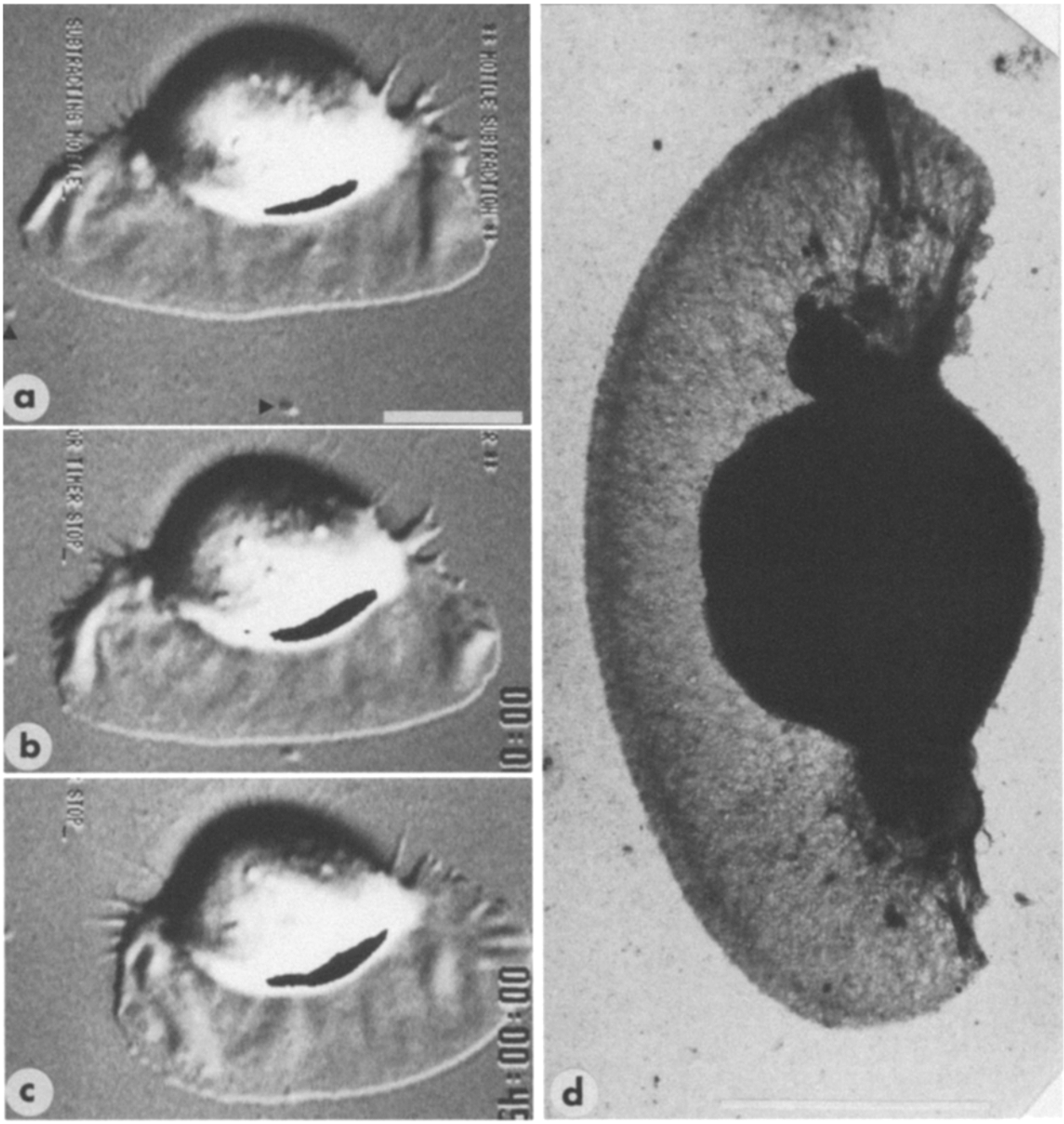

Figure 1. (*a–c*) Video-enhanced differential interference contrast images of a locomoting trout keratocyte taken at 3 time points: *a*, 0 s; *b*, 31 s; *c*, 55 s. Arrowheads point to stationary landmarks. Note constant fan-like shape and turning motion in *c*. (*d*) Electron micrograph of negatively stained keratocyte cytoskeleton showing uniform fan-like shape. Note also differentially stained fringe at cell front. Bars, 10 μm.

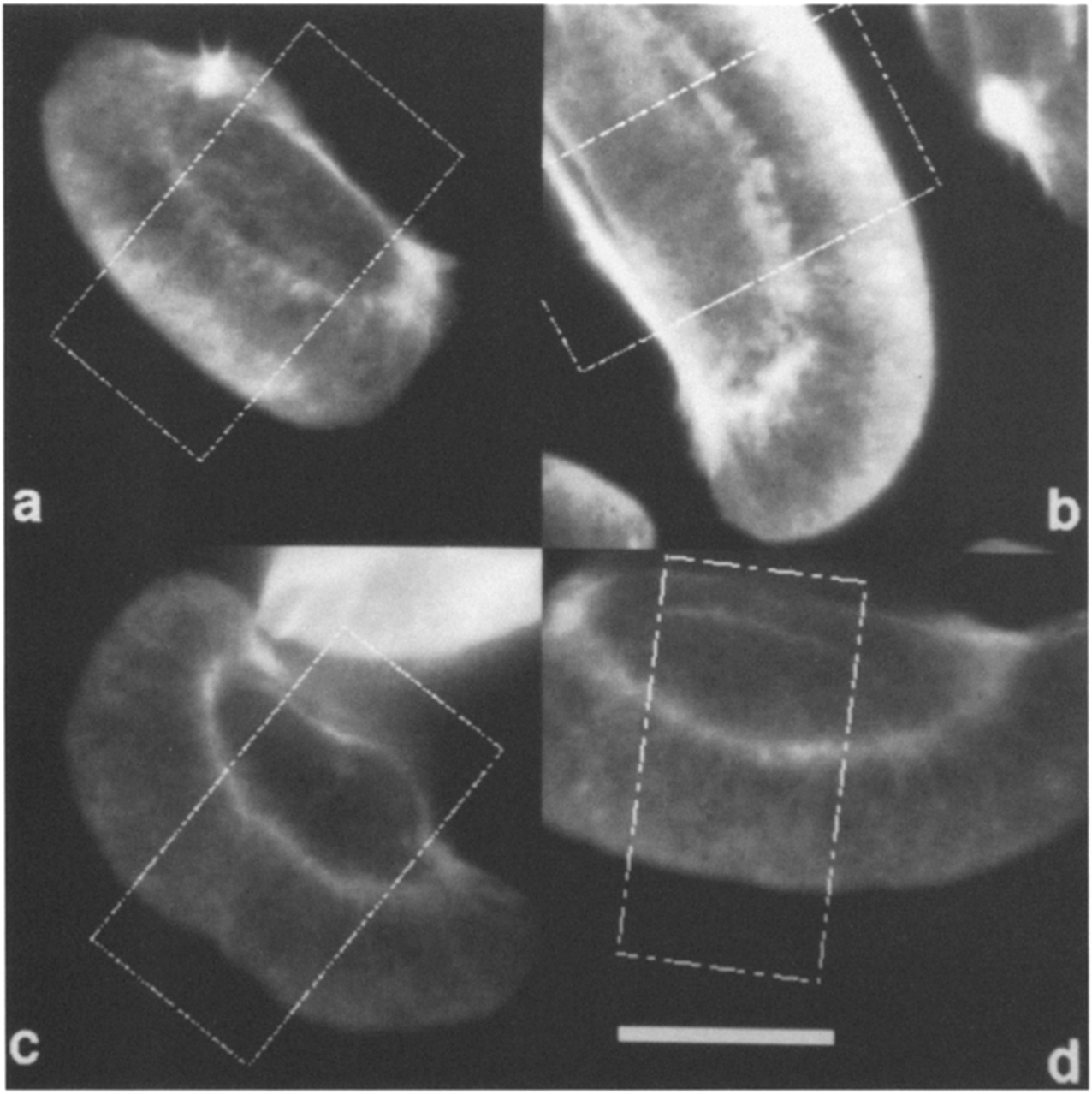
a
b
c
d

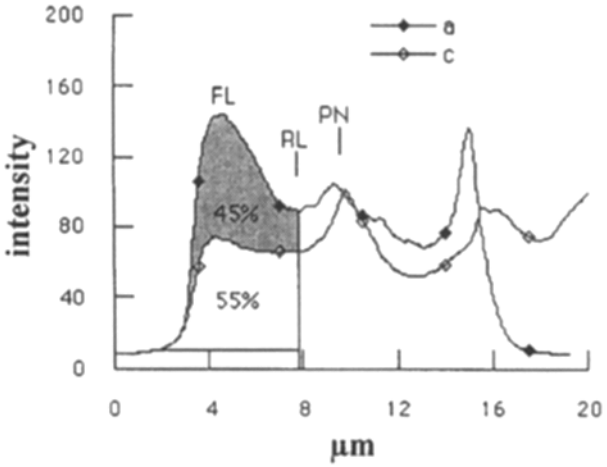
200
160
120
80
40
0
intensity
a
c
FL
RL
PN
45%
55%
0
4
8
12
16
20
µm

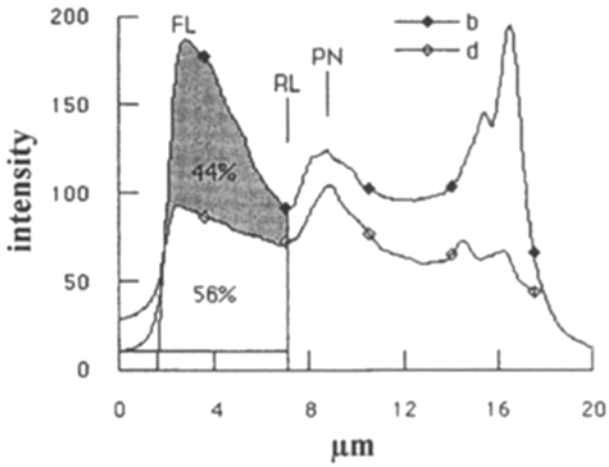
200
150
100
50
0
intensity
b
d
FL
RL
PN
44%
56%
0
4
8
12
16
20
µm

the periphery of the cell, the grids used for these experiments were floated on drops of 0.1% bovine serum albumin for one or more hours prior to the addition of tissue pieces. Cytoskeletons were also labeled with S-1 without the addition of exogenous actin. In this case S-1 was added after the first treatment with phalloidin.

Video-enhanced Interference Microscopy

Video microscopy with Nomarski interference optics was performed as described in Rinnerthaler et al. (1991) but at room temperature and using a simplified observation chamber comprised of a thin (0.7 mm), ring-shaped stainless steel spacer (inner diameter, 10 mm) sandwiched between a slide and a 20-mm diam coverslip carrying the cells. The sandwich was assembled with a thin layer of vacuum grease on the joining surfaces.

Fluorescence Microscopy and Intensity Scanning

Keratocytes were labeled with rhodamine-conjugated phalloidin (a gift from Prof. H. Faulstich, Max-Planck Institute, Heidelberg, Germany) after fixation at room temperature in one of the following three ways: (*a*) extraction with 0.5% Triton X-100 in MFR for 15 s, followed by 30-s fixation in 1% glutaraldehyde in MFR, and then a 30-min fixation in 3% paraformaldehyde in Tris-buffered saline (TBS: 20 mM Tris, 0.154 M NaCl, 2 mM $MgCl_2$, 2 mM EGTA, pH 7.5); (*b*) fixation in a mixture of 0.3% Triton X-100 and 3% paraformaldehyde in TBS or MFR for 30 min; and (*c*) fixation in 3% paraformaldehyde in TBS for 30 min followed by extraction in 0.5% Triton X-100 in MFR for 30 s. Phalloidin staining was performed by placing coverslips in 15-mm flat-bottomed wells containing 0.5 ml of 0.1 μg/ml rhodamine phalloidin in TBS. After staining overnight the coverslips were rinsed in TBS and mounted in Gelvatol containing 5 mg/ml *n*-propyl-gallate (Sigma, Munich, Germany).

Video images were acquired from a Zeiss Photomicroscope III (63× planapo objective, 4× TV tube, optovar 2×) using a Hamamatsu C-2400-87 image intensifier system and Argus 10 processor, operating in a 16-frame averaging mode, and transferred to a Macintosh Quadra 640 computer equipped with a Scion LG-3 frame grabbing card. All images were obtained under identical conditions, using a fixed gain on the intensifier, and a 3% neutral density filter on the microscope to reduce bleaching to negligible levels. The linearity of camera response over the range of grey scales measured was confirmed by measuring the attenuation produced by a supplementary set of neutral density filters. Digital images were scanned across a 10 × 20-μm box positioned near the middle of the lamellipodium, as normal as possible to both the edge of the cell and the edge of the perinuclear region using the public domain NIH Image program (written by Wayne Reasband at the U.S. National Institutes of Health and available from the Internet by anonymous ftp from zippy.nimh.nih.gov or on floppy disk from NTIS, Springfield, VA, part number PB93-504868). Plot values represent the average pixel value across the box versus distance from the box front. Final screen magnification was 6,700×, as determined using a Graticules (Tonbridge, England) stage micrometer slide with a 2-μm grating, projected onto the screen.

Results

Keratocyte Locomotion

Goodrich (1924) first described the characteristic shape and movements of fish keratocytes and this was re-emphasized in more recent work (Cooper and Schliwa, 1986; Kolega, 1986; Kucik et al., 1990; Theriot and Mitchison, 1991). For the present discussion we shall note that the remarkable feature of this cell type is not simply that it moves very fast but that it can do so without any significant change in shape. This is illustrated in the video series shown in Fig. 1 (*a–c*). Moving at speeds of around 10-μm/min these cells typically show a canoe-like shape (Goodrich, 1924), or appear as a cap, embracing the nuclear region, with a peak, corresponding to the lamellipodium. Goodrich used the general term "fan cells" to describe these cells and we shall adopt this term in the following. As can be seen in the video series there is effectively no change in shape of the fan cell during unobstructed movement. The changes that one does see include modulations in activity of the lateral edges of the lamellipodium, that lead to slight skewing movements of the cell. Thus, the cell steers itself by increasing the protrusive activity of one of its lateral edges at the expense of the other; this automatically leads to a shift in orientation of the lamellipodium as a whole and to a change in the direction of migration (Fig. 1 *c*).

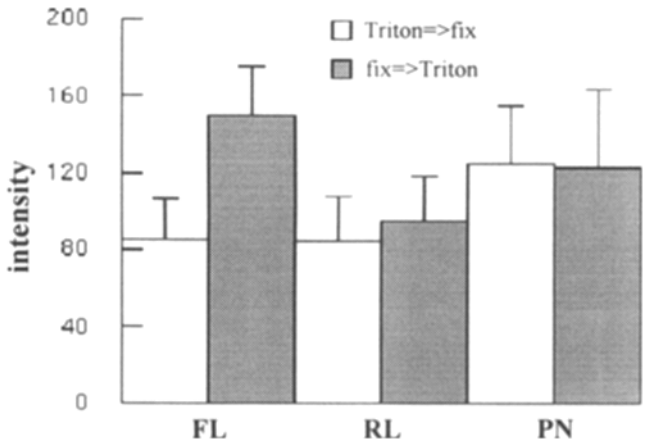

Figure 3. Average values for the fluorescence intensity of the front and rear of the lamellipodium (respectively, *FL* and *RL*) and for the perinuclear border (*PN*) in cells stained with fluorescent phalloidin and scanned as for Fig. 2. Empty bars are values for cells extracted with Triton and then fixed (*Triton-fix*) and shaded bars for cells fixed first and then extracted with Triton (*fix-Triton*). The data were derived from a total of 20 cells from each fixation and two separate experiments. Standard deviations are indicated by the error bars.

Fixation Dependence of Phalloidin Staining and Actin Filament Density

In line with previous studies of other cells (Small, 1981; Small et al., 1982) we tested the suitability of glutaraldehyde–Triton mixtures for producing keratocyte cytoskele-

Figure 2. (*a–d*) Video images of rhodamine phalloidin labeled keratocytes captured on a low light video camera. *a* and *b* are typical examples of cells that were first fixed and then extracted with Triton and *c* and *d* are corresponding examples of cells first extracted with Triton and then fixed (for exact conditions see Materials and Methods). The traces shown below each pair are the aligned scans of fluorescence intensity made across the boxed areas in the corresponding video images (*a–d*). Scans were paired from cells having lamellipodia of similar width which allowed a comparison of the total integrated intensity across the lamellipodium from the front (*FL*) to the rear (*RL*). Taking the integrated value for lamellipodia of cells that were first fixed as 100%, the two percentage values indicate the relative proportions of total stain remaining in the lamellipodia of Triton cytoskeletons (*b* and *d*, *unshaded region* between FL and RL) and, correspondingly, the proportion lost in Triton (*shaded region*), that is retained in the pre-fixed cells (*a* and *c*). *FL*, front of lamellipodium; *RL*, rear of lamellipodium; *PN*, perinuclear border. Bar, 10 μm.

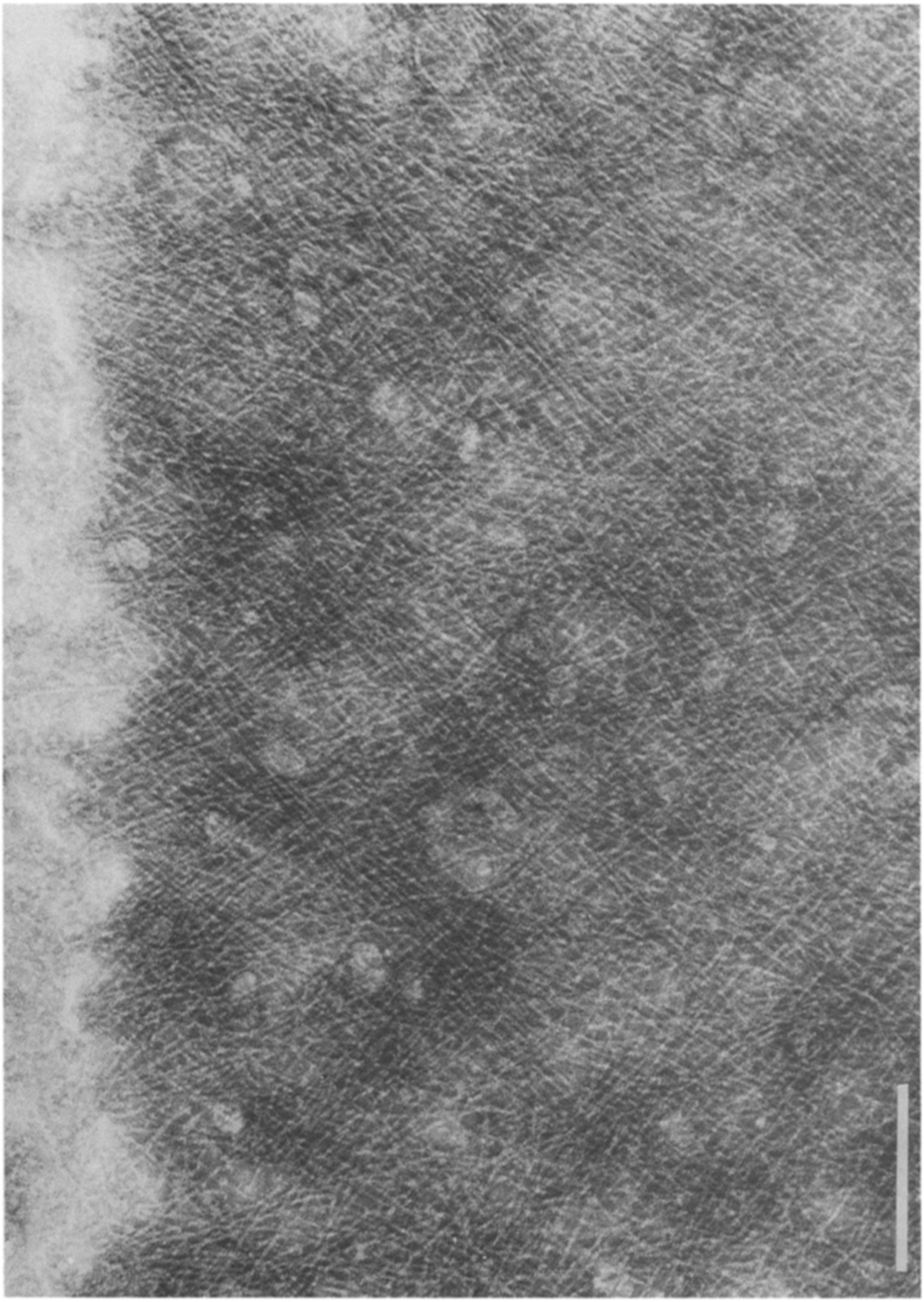

tons. The lamellipodium was however too dense in the electron microscope after such fixations for filaments to be easily visualized. The best visibility of filaments was achieved in keratocytes that were briefly extracted with Triton X-100 (0.5%, 15 s) and then fixed in glutaraldehyde. The question then arose as to whether the entire complement of actin filaments was preserved in the Triton cytoskeletons (see also Lewis and Bridgman, 1992). Before discussing the ultrastructural data it is pertinent to consider this problem first since it bears directly on the final conclusions drawn.

To establish the effects of the extraction procedure we measured the fluorescence intensity across lamellipodia of cells that were fixed according to different routines and then labeled with fluorescent phalloidin (Fig. 2). Intensity scans were made on images acquired directly from a low light video camera for which there was a linear response to intensity changes in the range of operation used (see Materials and Methods). Fig. 2 shows typical examples of cells prepared according to two procedures; one mimicking that used for electron microscopy (Triton followed by aldehyde: *c* and *d*) and the other for which we would expect no loss of actin filaments (aldehyde followed by Triton: *a* and *b*). In the latter case Triton treatment was necessary to facilitate the penetration of phalloidin. Scans of the fluorescence intensity made across lamellipodia of cells that were first fixed and then extracted, showed typically a high peak of intensity at the front followed by a steep fall-off to the rear (Fig. 2, traces *a* and *b*). In contrast, cells first extracted with Triton and then fixed showed much shallower profiles, with a relatively small or negligible decline in fluorescence intensity from the front to the rear of the lamellipodium (Fig. 2, traces *c* and *d*). The average values for the intensities at the front (FL) and rear (RL) of the lamellipodium and for the perinuclear region (PN) for 20 cells from each fixation are given in Fig. 3. As is seen in the figure, the major difference between the two preparations was in the peak intensity at the front of the lamellipodium which was on average 76% higher in the prefixed cells (shaded bars in Fig. 3).

A comparison of representative scan pairs (Fig. 2) of cells of similar size indicated that primary Triton extraction produced lamellipodia that retained roughly 55% of the total complement of filamentous actin, when compared to cells that were fixed before extraction. The scan profiles further showed that the major loss of actin filaments occurred progressively more towards the front of the lamellipodium. For cells fixed with a mixture of formaldehyde and Triton (see Materials and Methods) the intensity profile compared closely to that of pre-fixed cells (not shown).

Lamellipodium Ultrastructure in Triton Cytoskeletons

From the data in the previous section we conclude that the cytoskeletons of keratocytes obtained by brief Triton treatment retain somewhere around half or marginally more of the total complement of filamentous actin in the lamellipodium. In this section we will describe the ultrastructure of the keratocyte Triton cytoskeleton as observed after negative staining. A consideration of the missing complement of actin filaments will be reserved for the discussion.

At low magnification in the electron microscope the keratocyte lamellipodium appeared more or less homogeneous in density (Fig. 1 *d*); no microspike bundles were observed, but radial folds at the lateral flanks could sometimes be seen (Fig. 1 *d*). These folds corresponded to the radially oriented ruffles or pleats observed in the same position in some locomoting, living cells (see also Lee et al., 1992). In some cells we noted a fringe of different stain intensity at the front of the lamellipodium (e.g., Fig. 1 *d*) that ranged in width from 0.5–1.5 μm. At higher magnification, the striking feature of the lamellipodium was the close-to-regular, two dimensional order of actin filaments. To a rough approximation, the filaments were arranged in two orthogonal arrays that subtended an angle of around 45° with the cell front (Fig. 4). This arrangement was not as dramatic in small regions of the leading edge, necessarily depicted in selected figures (Fig. 4), as it was from general surveys in the electron microscope, or in micrograph montages too large to publish. The two sets of filaments in Fig. 4 can be best observed by tilting the micrograph at a glancing angle. Towards and around the curved ends of the lamellipodium the filament density at the cell edge decreased to 60–80% of that in the mid region and there was a noticeable increase in the range of angles subtended by actin filaments, relative to the local cell front (from around 20° to 160°). At the far, trailing borders of the lamellipodia fans, the cell edge was delimited by one or more bundles of actin filaments (seen at low magnification in Fig. 1 *d*). The radial folds sometimes observed in the lateral regions did not contain such bundles but consisted of folded actin meshworks (not shown).

An additional marked feature of the keratocyte cytoskeleton was the drop in filament density towards the rear of the lamellipodium. This is illustrated in Fig. 5, (*a–d*) which depicts selected images of a typical lamellipodium taken at progressively greater distances from the cell front (in this case at 0, 3, 6, and 9 μm, respectively). In the posterior, less dense regions of lamellipodia the filaments could be followed for considerable distances along their length (e.g., Fig. 6) and their orthogonal arrangement was still approximately preserved. In images such as Fig. 6 many filaments could be traced for up to 2.0 μm (average 1.58 ± 0.35 μm standard deviation for 20 filaments) before they became lost in the filament net. And in favorable instances we were able to trace single filaments over distances of up to 4 μm.

Fan cell lamellipodia varied considerably in width, from around 3–15 μm along a mid line in the cell parallel to the direction of movement. Nevertheless, there was always a consistent pattern of filament density change from front to

Figure 4. High magnification view of front of keratocyte lamellipodium. Note the predominant arrangement of filaments in two orthogonal arrays, each oriented at around 45° to the cell edge. The continuity of the filaments is best appreciated by viewing at a glancing angle. Negatively stained with a mixture of 1% sodium silicotungstate and 1% phosphotungstic acid. Bar, 0.25 μm.

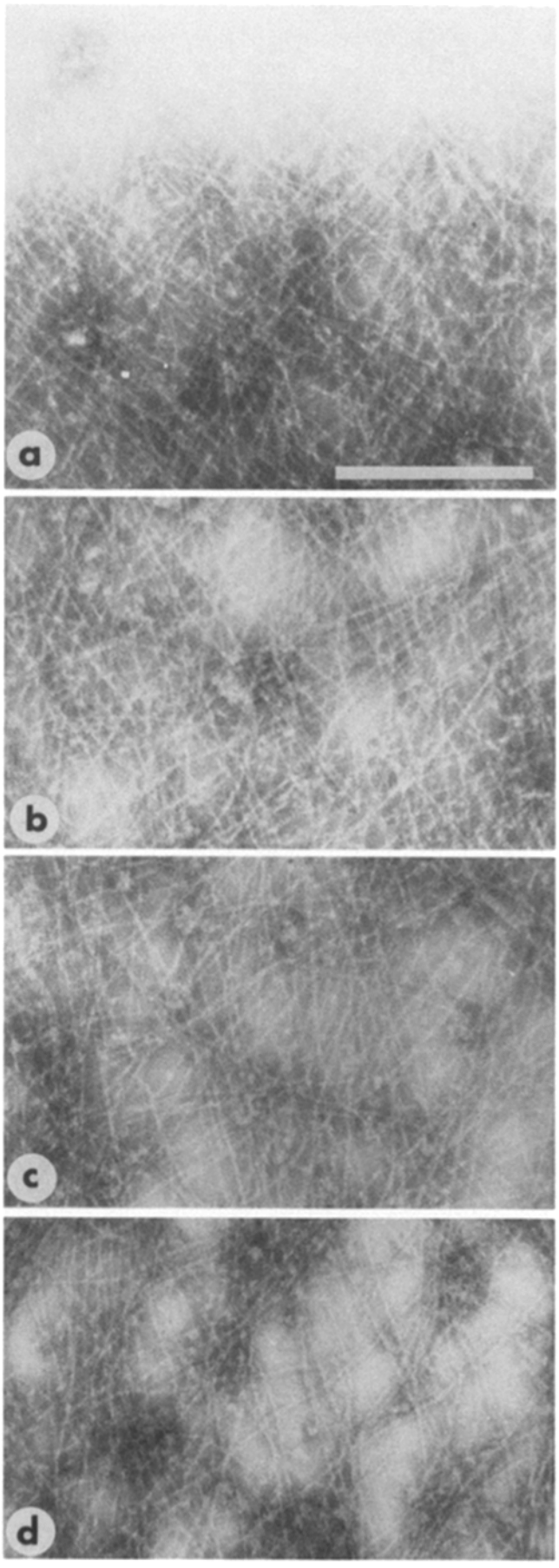

back. This is shown in Fig. 7 which presents the results of filament counts made at progressively posterior regions in three representative cells with lamellipodia of different width. Counts were made by recording the number of filaments crossing a line of 1 μm in length drawn parallel to and at a given distance from the cell front. The data showed that there was a more or less constant number of filaments in the anterior half of the lamellipodium of Triton cytoskeletons and a steady drop in filament density from the mid region to the perinuclear zone. We interpret this result as indicating a minimum filament length, spanning the first half of the lamellipodium, a maximum length spanning the distance from the cell front to the perinuclear region and intermediate lengths between these values. Since the filaments subtend an angle of around 45° to the cell front the longest will be in the range of 1.4 times the width of the lamellipodium in length. Free ends of filaments pointing in the direction of the front edge of the lamellipodium were not found, neither were short filaments detected in the more open regions of the actin networks.

Actin Filament Polarity

Decoration of lamellipodia cytoskeletons with myosin S-1 followed by negative staining, resulted in the deposition of too much electron-dense stain for the arrowhead pattern on the meshwork filaments to be distinguished. Attempts were made to visualize the arrowhead polarity using quick freeze deep-etching (see Lewis and Bridgman, 1992) but in the dense actin networks of the keratocyte we were unable to determine the arrowhead direction, even though the filaments were clearly decorated (Small J. V., M. Häner, and U. Aebi, unpublished observations). We therefore adopted another approach. Thus, exogenously added actin was polymerized onto lightly fixed keratocyte cytoskeletons to produce an actin fringe, which was then decorated with S-1. In this way we could show that all filaments seeded onto the anterior edge of the lamellipodium had their fast-growing, plus ends directed outwards (Fig. 8).

Discussion

To develop their nucleation release model for the keratocyte Theriot and Mitchison (1991) took as a key piece of data the distribution of phalloidin label across the lamellipodium, which they found to be homogeneous. As we show, the staining of the lamellipodium with phalloidin varies considerably according to the method of fixation. Theriot and Mitchison (1991) do not state precisely how they fixed their keratocytes but only in cells pre-extracted with Triton did we find a flattened distribution of phalloidin stain approaching that which they describe. We conclude that these authors had lost, in their phalloidin-labeled cells, the extra component of actin seen in pre-

Figure 5. Images of the actin meshwork in a wide keratocyte lamellipodium taken at progressively greater distances from the front edge: *a*, 0 μm; *b*, 3 μm; *c*, 6 μm; *d*, 9 μm. Note drop in filament density towards the rear of the lamellipodium. Negatively stained with 1% sodium silocotungstate. Bar, 0.25 μm.

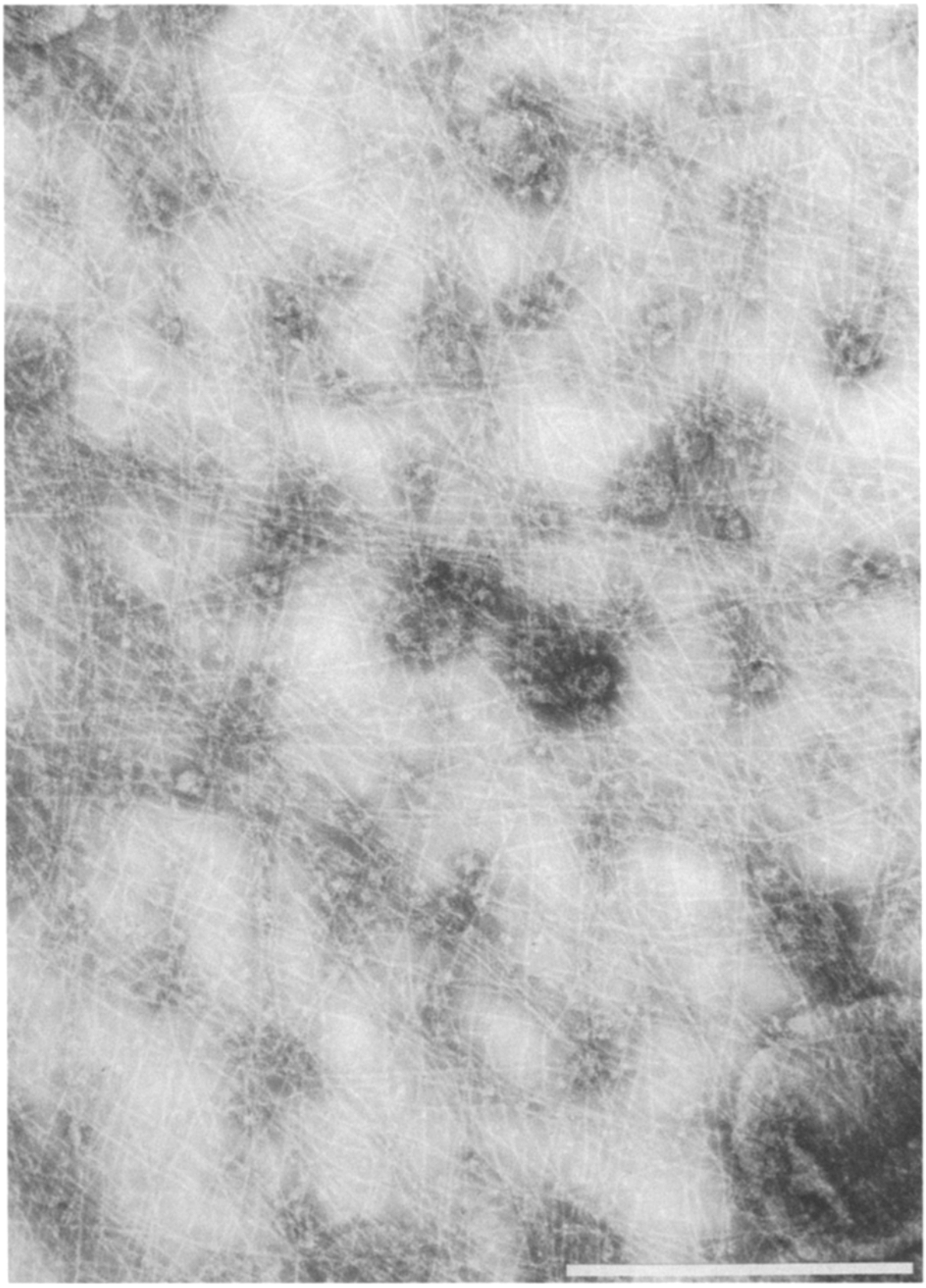

Figure 6. Actin meshwork in inner lamellipodium region in which the length of the filaments (extending beyond the borders of the micrograph) can be better appreciated. Note also approximately orthogonal arrangement. Negatively stained with 1% sodium silocotungstate. Bar, 0.5 μm.

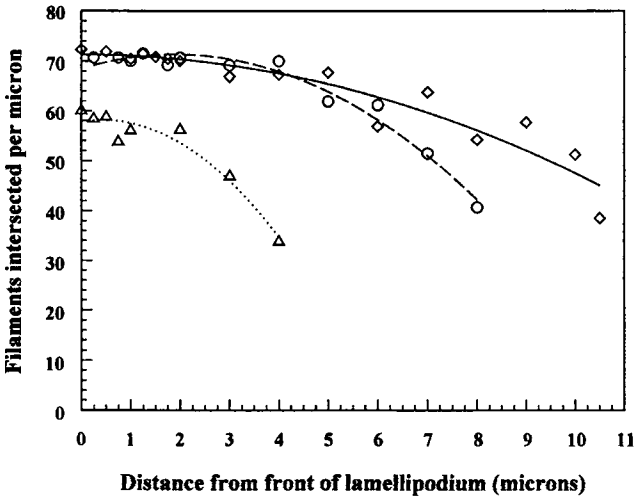

Figure 7. Change in filament density from the front to the rear of three typical lamellipodia of different width, expressed in terms of filament counts. Each point represents the number of filaments transected by a 1-μm long line drawn on enlarged micrographs parallel to and at the distance from the front edge indicated.

fixed preparations, and thus failed to detect the steep gradient of filament density that exists across the lamellipodium. Had they observed this gradient they would not have found their data on activated fluorescence at variance with a treadmilling type mechanism (see also below).

Turning now to the ultrastructural data, we observed in Triton cytoskeletons a semi-ordered criss-cross organization of long actin filaments, oriented in the middle front part of the lamellipodium at around 45° to the cell edge. Indeed, a criss-cross arrangement of actin filaments in the keratocyte was suggested by earlier fluorescence micrographs of these cells labeled with phalloidin (Cooper and Schliwa, 1986; Heath and Holifield, 1991*b*). The same criss-cross arrangement can be observed in fibroblasts (Small, 1981; Small et al., 1982) and is characteristic of lamellipodia that are actively protruding (Small, J. V., unpublished observations). Although we could not trace single filaments from the front to the back of the lamellipodium we could follow them over many microns, in particular in the more posterior regions of the cytoskeleton. Taking the more or less ordered orthogonal arrangement of filaments and the steady drop in filament density in the latter half of the lamellipodium, we conclude that the filaments in Triton cytoskeletons have graded lengths ranging from around 4–15 μm or more, the range depending on the width of the lamellipodium.

It may be noted that the drop in filament number deduced from the electron micrographs was somewhat steeper than the drop in intensity of phalloidin label in the Triton cytoskeletons. The source of this difference is not clear but it could derive from a collapse of the perinuclear region after Triton extraction that causes a spread of phalloidin label into the base of the lamellipodium. An equivalent phenomenon may not occur in the electron microscope preparations due to a shrinkage of the perinuclear region on drying.

The phalloidin-labeling data demonstrates that Triton cytoskeletons prepared in the way described retain only marginally more than half of the total complement of F-actin in the lamellipodium. In trying to determine the organization of the component lost in Triton we analyzed cells that were pre-fixed in glutaraldehyde and then extracted with Triton and negatively stained. The increased density of material observed in the lamellipodium was consistent with the retention of an extra complement of actin, but structural details were difficult to resolve.

However, in preparations incubated for long periods in the negative stain solution prior to drying, we could discern a criss-cross arrangement of filaments at the front of the lamellipodium similar to that seen in Triton cytoskeletons (not shown). A possible explanation of these findings is that the lamellipodium has a stratified organization, featuring two sets of actin filaments, one associated with the ventral and the other with the dorsal membrane. Since the ventral set is probably bound indirectly to the substrate it would be more resistant against extraction by Triton, whereas a dorsal set could be readily removed. The dorsal set need not differ significantly in organization from that on the ventral side (and that we have observed in the electron microscope), but according to the phalloidin labeling data would probably feature filaments with a smaller range of lengths. This would not be unexpected since the upper set would probably terminate before the lamellipodium curves upwards at the rear into the perinuclear region (Bereiter-Hahn et al., 1981) while the ventral set may extend into the space beneath the perinuclear border where the membrane remains flat. Some of our future attention must focus on clarifying the interrelationships and functions of the extractable and stable components of actin filaments in the lamellipodium.

In the latter context it is interesting to note that Lewis and Bridgman (1992) concluded, in an electron microscope study of neuronal growth cone cytoskeletons, that a cortical layer of filaments may be lost on Triton treatment, consistent with the present findings on keratocytes. But the same authors draw two further conclusions that are not in line with our own interpretations. First, they claim to detect two populations of actin filaments in growth cones, longer filaments that are sometimes bundled and, between these, shorter filaments that are randomly arranged. Given the difficulties of tracking single filaments along their entire length in deep negative stain the "short" filaments they observe could just as well be long filaments that over or underlap other filaments and bundles in the lamellipodium. As we note elsewhere (Small et al., 1994) neither negative staining nor freeze drying and shadowing offers the ideal solution for determining filament length. However, the presence of two dimensional order in the keratocyte cytoskeleton provides, in our view, a more compelling argument for a single population of filaments. A second issue concerns the polarity of actin filaments in the lamellipodium. For the neuronal growth cone, Lewis and Bridgman (1992) show actin filaments with their barbed ends pointing both towards and away from the cell front. But, as these authors note, like others previously, the rear edge of the lamellipodium is marked by the rear ends of the larger filament bundles that span the lamellipodium and that are commonly found in cultured tissue cells. By this criterion, Lewis and Bridgman (1992) show

decorated filaments that are not in the true lamellipodium, but behind it where the actin filaments are arranged in more open and random networks (Rinnerthaler et al., 1992). The claim (Lewis and Bridgman, 1992) that filaments in the lamellipodium have variable polarity cannot therefore be made from these findings.

From the present structural data on keratocytes we conclude that actin filaments abut the anterior edge of the lamellipodium with their fast growing plus ends, and extend rearwards to different extents, up to 15 μm or more towards the perinuclear zone. Since we were unable to map the polarity of filaments in the body of the lamellipodium we cannot rigorously exclude the possibility that free plus ends of actin filaments exist also behind the anterior edge, although we consider this unlikely. Our conclusion that the plus end are exclusively at the front and the minus ends distributed over the lamellipodium according to the fall off in filament density will require confirmation by other techniques. The use of probes that specifically mark plus and minus filament ends may help resolve this issue. For the time being we will only draw attention to the fact that all of the data so far available on the keratocyte is consistent with a mechanism of locomotion of the treadmilling type (Wang, 1985), with growth of fast actin filament ends at the anterior edge of the lamellipodium and breakdown or depolymerization of filaments across most of the lamellipodium width, giving rise to filaments of graded length. The data of Theriot and Mitchison (1991) would be fully consistent with the same type of mechanism if the decay in activated fluorescence matches the decay in

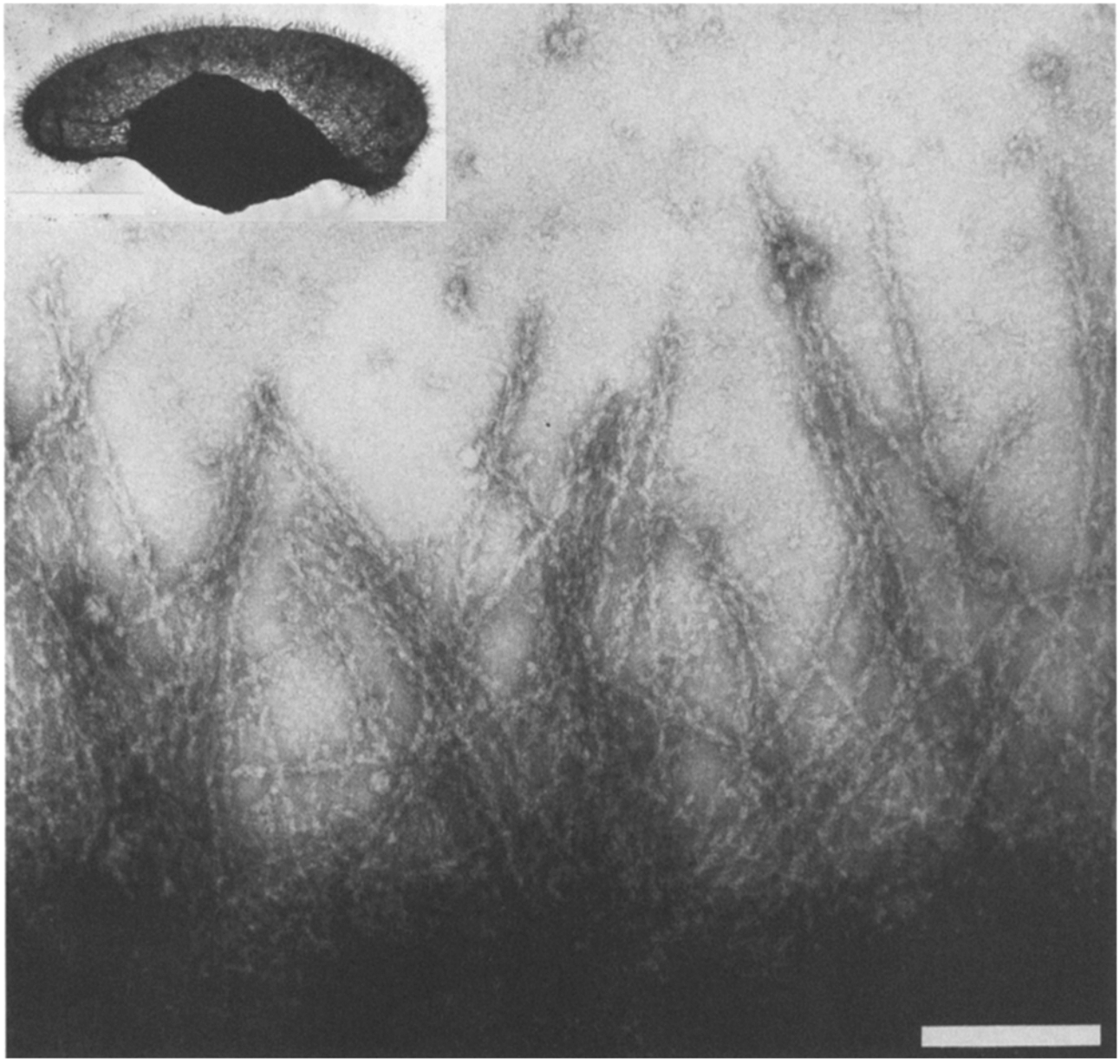

Figure 8. Polarity of actin filaments at the cell front. Micrograph shows keratocyte cytoskeleton that was incubated with actin monomers to induce growth of actin filaments beyond the front edge and then decorated with myosin S-1. Inset shows actin fringe at low magnification. Note uniform polarity of arrowheads with the barbed ends directed outwards. Bar, 0.25 μm; inset, 10 μm.

filament density, as deduced by phalloidin staining. From a visual inspection of Theriot and Mitchison's images we would predict that this would be the case, but parallel measurements of activated fluorescence and phalloidin labeling should ideally be made on the same cell.

What actually produces the force to protrude the advancing membrane is still a matter of some debate (Bray, 1992; Adams and Pollard, 1989; Smith, 1988; Mitchison and Kirschner, 1988; Peskin et al., 1993; Stossel, 1993; Small, 1993; Sheetz, 1994) but whatever it is, actin would appear to form an indispensible space filling role by undergoing vectorial polymerization to match the membrane advance. Gel-swelling models are rendered unlikely from the density of the filament network, which is high at the front (where it should be swelling; Condeelis, 1993) and lower at the rear. More plausible are models involving myosin I, since members of this motor family have been found in the lamellipodia of amoeba (Fukui et al., 1989) and vertebrate cells (Wagner et al., 1991). And directed motility with such motors would require an ordered and polarized framework of actin filaments, which we indeed find in lamellipodia.

We thank Dr. T. Mitchison for valuable discussion and constructive criticism of the manuscript, Dr. Yu-Li Wang for helpful advice on video microscopy and Dr. R. Cross and Prof. B. Geiger for useful comments. The referees of this work are likewise acknowledged for their pointed and helpful criticisms. We thank Ms. A. Rohlfs and Ms. B. Mies for technical assistance during different phases of this project and Mr. A. Weber for photography. Thanks also go to Prof. M. Schliwa and Dr. U. Euteneuer for helpful tips about culturing keratocytes and to Fischerei Bayerhammer for a generous and free supply of trout. We also thank Ms. E. Eppacher for typing.

Some of the instrumentation used in this project was provided in part by earlier grants from the Austrian Science Foundation.

Received for publication 10 October 1994 and in revised form 17 February 1995.

References

Abercombie, M., J. E. M. Heaysman, S. M. Pegrum. 1970. The locomotion of fibroblasts in culture. *Exp. Cell Res.* 59:393–398.

Adams, R. J., and T. D. Pollard. 1989. Membrane-bound myosin-I provides new mechanisms in cell motility. *Cell Motil. & Cytoskel.* 14:178–182.

Bereiter-Hahn, J., R. Strohmeier, I. Kunzenbacher, K. Beck, and M. Vöth. 1981. Locomotion of Xenopus epidermal cells in primary culture. *J. Cell Sci.* 52:289–311.

Bray, D. 1992. Cell movements. Garland Publishing Inc., New York. Pg. 152.

Cano, M. L., D. A. Lauffenburger, and S. H. Zigmond. 1991. Kinetic analysis of F-actin depolymerization in polymorphonuclear leukocyte lysates indicates that chemoattractant stimulation increases actin filament number without altering the filament length distribution. *J. Cell Biol.* 115:677–687.

Carlier, M.-F., and D. Pantaloni. 1994. Actin assembly in response to extracellular signals: role of capping proteins, thymosin β_4 and profilin. *Semin. Cell Biol.* 5:183–191.

Condeelis, J. 1993. Understanding the cortex of crawling cells: insights from *Dictyostelium*. *Trends Cell Biol.* 3:371–376.

Cooper, M. S., and M. Schliwa. 1986. Motility of cultured fish epidermal cells in the presence and absence of direct current electric fields. *J. Cell Biol.* 102: 1384–1399.

Edds, K. T. 1977. Dynamic aspects of filopodial formation by reorganization of microfilaments. *J. Cell Biol.* 73:479–491.

Forscher, P., and S. J. Smith. 1988. Actions of cytochalasins on the organization of actin filaments and microtubules in a neuronal growth cone. *J. Cell Biol.* 107:1505–1516.

Fukui, Y., T. J. Lynch, H. Brzeska, and E. D. Korn. 1989. Myosin I is located at the leading edges of locomoting *Dictyostelium* amoebae. *Nature (Lond.).* 341:328–331.

Goodrich, H. B. 1924. Cell behaviour in tissue cultures. *Biol. Bull (Woods Hole).* 46:252–262.

Heath, J. P., and B. F. Holifield. 1991*a*. Cell locomotion: new research tests old ideas on membrane and cytoskeletal flow. *Cell Motil. & Cytoskeleton.* 18: 245–257.

Heath, J. P., and B. F. Holifield. 1991*b*. Actin alone in lamellipodia. *Nature (Lond.).* 352:107–108.

Höglund, A. S., R. Karlsson, E. Arro, B. F. Fredriksson, and U. Lindberg. 1980. Visualization of the peripheral weave of microfilaments in glia cells. *J. Muscle Res. Cell Motil.* 1:127–146.

Karlsson, R., I. Lassing, A.-S. Höglund, and U. Lindberg. 1984. The organization of microfilaments in spreading platelets: a comparison with fibroblasts and glial cells. *J. Cell. Physiol.* 121:96–113.

Kolega, J. 1986. Effects of mechanical tension on protrusive activity and microfilament and intermediate filament organization in an epidermal epithelium moving in culture. *J. Cell Biol.* 102:1400–1411.

Kucik, D. F., E. L. Elson, and M. P. Sheetz. 1990. Cell migration does not produce membrane flow. *J. Cell Biol.* 111:1617–1622.

Lee, J., A. Ishihara, and K. Jacobson. 1993. How do cells move along surfaces? *Trends Cell Biol.* 3:366–370.

Lee, J., A. Ishihara, J. A. Theriot, and K. Jacobson. 1993. Principles of locomotion for simple-shaped cells. *Nature (Lond.).* 362:167–171.

Lewis, A. K., and P. C. Bridgman. 1992. Nerve growth cone lamellipodia contain two populations of actin filaments that differ in organization and polarity. *J. Cell Biol.* 119:1219–1243.

Mitchison, T., and M. Kirschner. 1988. Cytoskeletal dynamics and nerve growth. *Neuron.* 1:761–772.

Moore, P. B., H. E. Huxley, and D. J. De Rosier. 1970. Three dimensional reconstruction of F-actin, thin filaments and decorated thin filaments. *J. Mol. Biol.* 50:279–295.

Okabe, S., and N. Hirokawa. 1989. Incorporation and turnover of biotin-labeled actin microinjected into fibroblastic cells: an immunoelectron microscopic study. *J. Cell Biol.* 109:1581–1595.

Okamoto, Y., and T. Sekine. 1985. A streamlined method of subfragment one preparation from myosin. *J. Biochem.* 98:1143–1145.

Oster, G. F., and A. S. Perelson. 1987. The physics of cell motility. *J. Cell Sci.* 8: 35–54.

Peskin, C. S., G. M. Odell, and G. F. Oster. 1993. Cellular motions and thermal fluctuations: the brownian ratchet. *Biophys. J.* 65:316–324.

Rinnerthaler, G., M. Herzog, M. Klappacher, H. Kunka, and J. V. Small. 1991. Leading edge movement and ultrastructure in mouse macrophages. *J. Struct. Biol.* 106:1–16.

Small, J. V. 1981. Organization of actin in the leading edge of cultured cells; influence of osmium tetroxide and dehydration on the ultrastructure of actin meshworks. *J. Cell Biol.* 91:695–705.

Small, J. V. 1988. The actin cytoskeleton. *Electron Microsc. Rev.* 1:155–174.

Small, J. V. 1989. Microfilament-based motility in non-muscle cells. *Curr. Opin. Cell Biol.* 1:75–79.

Small, J. V. 1994. Lamellipodia architecture: actin filament turnover and the lateral flow of actin filaments during motility. *Semin. Cell Biol.* 5:157–163.

Small, J. V., and J. E. Celis. 1978. Filament arrangements in negatively stained cultured cells: the organization of actin. *Eur. J. Cell Biol.* 16:308–325.

Small, J. V., G. Isenberg, and J. V. Celis. 1978. Polarity of actin at the leading edge of cultured cells. *Nature (Lond.).* 272:638–639.

Small, J. V., G. Rinnerthaler, and H. Hinssen. 1982. Organization of actin meshworks in cultured cells: the leading edge. *Cold Spring Harb. Symp. Quant. Biol.* 46:599–611.

Small, J. V., A. Rohlfs, and M. Herzog. 1993. Actin and cell movement. *In* Cell Behaviour: Adhesion and Motility (G. Jones, C. Wigley, and R. Warn, editors). The Company of Biologists Ltd., Cambridge. 57–71.

Small, J. V., M. Herzog, M. Häner, and U. Aebi. 1994. Visualization of actin filaments in keratocyte lamellipodia: negative staining compared with freeze drying. *J. Struct. Biol.* 113:135–141.

Smith, S. J. 1988. Neuronal cytomechanics: the actin-based motility of growth cones. *Science (Wash. DC).* 242:708–715.

Spudich, J. A., and S. Watt. 1971. The regulation of rabbit skeletal muscle contraction. *J. Biol. Chem.* 246:4866–4871.

Stossel, T. P. 1993. On the crawling of animal cells. *Science (Wash. DC).* 260: 1086–1094.

Symons, M. H., and T. J. Mitchison. 1991. Control of actin polymerization in live and permeabilized fibroblasts. *J. Cell Biol.* 114:503–513.

Theriot, J. A. 1994. Regulation of the actin cytoskeleton in living cells. *Semin. Cell Biol.* 5:193–199.

Theriot, J. A., and T. J. Mitchison. 1991. Actin microfilament dynamics in locomoting cells. *Nature (Lond.).* 352:126–131.

Theriot, J. A., and T. J. Mitchison. 1992*a*. The nucleation–release model of actin filament dynamics in cell motility. *Trends Cell Biol.* 2:219–222.

Theriot, J. A., and T. J. Mitchison. 1992*b*. Comparison of actin and cell surface dynamics in motile fibroblasts. *J. Cell Biol.* 119:367–377.

Wagner, M. C., B. Barylko, and J. P. Albanesi. 1992. Tissue distribution and subcellular localization of mammalian myosin I. *J. Cell Biol.* 119:163–170.

Wang, Y.-L. 1985. Exchange of actin subunits at the leading edge of living fibroblasts: possible role of treadmilling. *J. Cell Biol.* 101:597–602.

Yin, H., and J. H. Hartwig. 1988. The structure of the macrophage skeleton. *J. Cell Sci.* 9 (Suppl.):169–184.

Zigmond, S. H. 1993. Recent quantitative studies of actin filament turnover during cell locomotion. *Cell Motil. & Cytoskeleton.* 25:309–316.